MEMS mirrors using sub-wavelength High-Contrast-Gratings with asymmetric unit cells

Milan Maksimović

***Abstract*—High-contrast gratings (HCG) are ultra-thin elements operating in sub-wavelength regime with the period of the grating smaller than the wavelength and with the high-index grating material fully surrounded by low-index material. Design of MEMS mirrors made from HCG with specific reflectivity response is of great practical interest in integrated opto-electronics. We theoretically investigate design of the spectral response for HCGs with the complex unit cells. We show that the spectral response can be tailored via the unit cell perturbations and with the asymmetric unit cell perturbations may introduce completely new spectral response. Our results can serve as guidance for the design of the complex HCGs and help with the choice of the efficient initial grating topology prior to global optimization procedure.**

***Index Terms*—High index contrast, subwavelength grating, MEMS, optical phased array.**

Original Research Paper
DOI: 10.7251/ELS1519052M

I. INTRODUCTION

THE optical grating is an important and widespread element used for manipulating or tailoring the spatial, temporal and spectral properties of light. A new type of high-contrast gratings (HCG) has been proposed recently, see [1]. HCGs are ultra-thin elements operating in the sub-wavelength regime, with a period of the grating smaller than the wavelength and with high-index grating material fully surrounded by low-index material. These structural characteristics of HCGs give rise to a variety of novel features with a great importance in integrated optoelectronics such as: ultra-broadband high reflectivity, high-quality-factor resonances, wave front phase control for planar focusing reflectors and lenses in integrated optics, etc. [1]-[4].

The motivation for extensive research in the manufacturing and design of HCGS and for their practical use has been to obtain an alternative for the distributed Bragg reflectors (DBR) for broadband high-reflectivity filtering applications [2]-[5]. The nature of HCGs dictates that their spectral response is very dependent on the polarization and as such it is applied for polarization control filters [6]. Also, novel ultra-low loss hollow-core waveguides are possible with the use of two HCGs as highly reflectivity mirrors [7]. Very interesting recent results emphasize the use of non-periodical and non-uniformly scaled HCG to imprint local phase shift onto an incident wave and to achieve focusing on a very small scale [8-9].

Modeling of HCGs can be effectively performed by numerous numerical methods for modeling optical response of gratings [10]. In this paper, we perform numerical simulations using the well known rigorous coupled wave analysis (RCWA) [11] in our own implementation. An important aspect of modeling HCGs is the use of different approximation methods, loosely named coupled-mode theory, that reveal some insight into the peculiar nature of HCGs electromagnetic response [12]-[16].

Another important technology is MEMS (micro-electromechanical systems), because it enables the application of silicon fabrication technologies to the development of micro optical elements in general [17],[18]. Fabrication of HCGs as MEMS mirrors structures or other integrated opto-electronics elements has been demonstrated [1].

Design and optimization of specific spectral, angular or spatial characteristics for periodic HCGs is of great practical interest. Recently, we investigated modeling and optimization of 1D HCGs with a periodic grating structure but with a complex unit cells topology [19]-[20]. The main emphasis of our paper is on the theoretical analysis suitable for the design of HCGs with prescribed spectral properties such as broadband reflection or high-Q resonances. In our approach, optimization tasks could be facilitated if we start with a design that already possesses the desired features .

In this paper, we further exemplify our method for spectral tailoring with the perturbations of the HCGs unit cell topology. We start with an analysis of the periodic HCGs supporting high broadband reflectance. Second, structural perturbations in the form of deformed unit cells are introduced into the simple periodic structures already optimized for the specific broadband response. Third, we analyze reflection/transmission resonances in the structure where the unit cell is symmetrically or asymmetrically perturbed. In the examples we provide, the role of the unit cell symmetry is revealed as the origin of spectral resonances. Finally, we make some comments on further applications of HCG mirrors for tailoring phase response.

II. HIGH CONTRAST GRATINGS MODELING

A. Modeling HCGs with general methods

The common form of HCG is a periodic array of rectangular high-index bars surrounded by low index material.

Manuscript received 12 October 2015 (write the date when you have first sent the manuscript for review). Received in revised form 20 October 2015 (write the date when you have sent the manuscript in its revised form if revisions required for your paper after review).

Milan Maksimović is with the Focal-Vision and Optics, Enschede, The Netherlands (corresponding author to provide phone: +31-053-4287-885; e-mail: milan.maksimovic@focal.nl).

The HCG is excited by plane wave excitation with defined polarization and under a normal or oblique incidence angle. The period of the grating structure is smaller than the wavelength of the incoming wave and hence the HCG is sub-wavelength. This means that only the zeroth diffraction order mode is propagating outside the grating region. In the case of oblique incidence the sub-wavelength operating condition of $\Lambda > \lambda$ is replaced by $(1+\sin\theta)\,\Lambda > \lambda$ for oblique incidence.

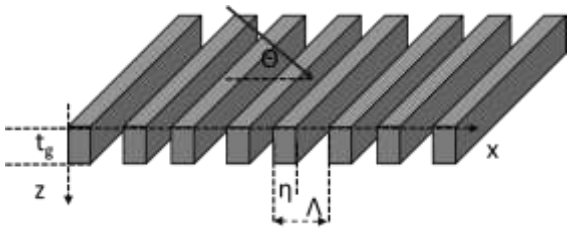

Figure 1 Basic geometry of high index contrast grating with a unit cell period Λ and high index bar width i ηΛ, where η is the duty cycle of the grating and t_g is the grating height. The structure is periodic in the x-direction, and is infinitely extended in the y direction with the plane wave incident from the top under an incidence angle Θ.

The structure depicted in Figure 1 is invariant along the y-direction and illuminated by the incident plane wave under an angle Θ. The electromagnetic field can be decomposed into two different polarizations TE (with E_y,H_x,H_z the only non-null components) and TM (with H_y,E_x,E_z the only non-null components). The wave equations can be written in the compact form:

$$\mathbf{L}_{\mathrm{TE(TM)}}\Phi(x,z) = -\frac{1}{k^2}\partial_z^2\Phi(x,z), \qquad (1)$$

with Φ(x,z) representing either E_y or H_y component depending on polarization. The operator **L** is defined as:

$$\mathbf{L}_{\mathrm{TE}} = \frac{1}{k^2}\partial_z^2 + \mathrm{n}^2(x), \qquad (2)$$

$$\mathbf{L}_{\mathrm{TM}} = \frac{1}{k^2}\mathrm{n}^2(\mathrm{x})\,\partial_x \frac{1}{\mathrm{n}^2(\mathrm{x})}\partial_x + \mathrm{n}^2(\mathrm{x}), \qquad (3)$$

with k=2π/λ and n(x) being the refractive index distribution. Since the operator **L** does not depend on the z-variable, the separation of variables leads to the representation

$$\Phi(x,z) = \varphi(x)e^{\pm ikz} \qquad (4)$$

where φ is the eigenfunction for corresponding eigenvalue problem

$$\boldsymbol{L}_{TE(TM)}\varphi(x) = r^2\varphi(x) \qquad (5)$$

Owing to the periodicity of the structure the eigenfunctions are pseudo-periodic $\varphi(x+\Lambda) = \varphi(x)e^{\pm ik\alpha\Lambda}$ with $\alpha = \sin(\Theta)$ determined by the incidence angle while the square root of the eigenvalue is chosen in such way that $Im(r) < 0$ or $r > 0$ if the eigenvalue is real. The solutions in the exterior of the grating can be expressed in terms of propagating and evanescent plane wave components

$$\Phi_{IN}(x,z) = \Phi_{inc}(x,z) + \textstyle\sum_m r_m e^{-i(k_x x + k_z z)}, \qquad (6)$$

$$\Phi_{OUT}(x,z) = \textstyle\sum_m t_m e^{-i\left(k_x x + k_z (z - t_g)\right)}, \qquad (7)$$

where r_m,t_m are reflection and transmission coefficients. Owing to the periodicity of the geometry and the fact that the grating is homogeneous in the propagation direction (z-axis), the permittivity and the field components can be represented by Fourier expansion. Further, boundary conditions are used for the neighboring regions to form a matrix representation and enable the calculation of the coupling coefficient for each Fourier component. This mathematical method is known as the rigorous coupled wave analysis method (RCWA) and it has been widely applied in solving grating problems of different complexity [10]-[11]. Furthermore, the symmetry of the structure plays an important role in the form of general solution. HCG has a standard discrete and continuous translations symmetry but additional symmetries such as mirror symmetry of the unit cell may further restrict the solution to the full problem. Other general purpose methods such as finite element method (FEM) or finite difference time domain (FDTD) method can be used to model HCG structures, see [11] for an overview.

B. Modeling HCGs: coupled mode theory (CMT)

There are several semi-analytical, approximate methods relying on an expansion of the fields in the grating region in a specially chosen basis. These formalisms rely on the expansion using periodic waveguide modes as the basis for the field representation in the grating region and have been developed in several versions under the name as the coupled mode [1], [13] or the coupled Bloch-mode method [12]. Another version of the coupled mode approach has been derived in [15].

An essential part of the method is to identify waveguide modes in the grating region and their interaction as responsible for transfer of energy across the grating [1],[13],[14]. Many interesting physical effects can be understood in terms of resonant excitation of leaky modes (Bloch modes of periodic waveguide) supported by the structure. Under normal incidence the excitation of two coupled Bloch-modes and their destructive interference are responsible for the spectral properties of HCGs such as broadband reflection. In the case of oblique incidence more complicated interactions that include different and numerous waveguide modes are important.

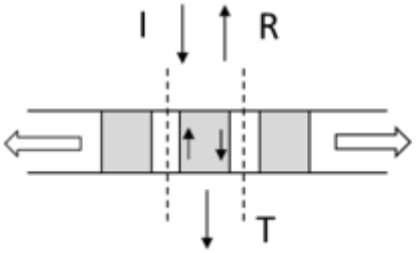

Figure 2 Sketch of the high index contrast grating with depiction of excited waveguide modes in the grating region. Interference of these modes is responsible for all properties of HCGs.

Further, in the deep subwavelength region the Effective Medium Theory is a very useful tool [12], while its applicability relies on the excitation of a single propagating mode. Hence, it does not predict the features of the spectral response for HCGs in the case where (small) number of modes

is excitable. In the case of simple structures these CMT and similar approaches offer valuable insights into the physics of HCGs, but as pure numerical methods they do not outperform the standard RCWA in terms of convergence properties for more complex structures and across full parameter space [1]. In addition, these methods can give an insight into the design with the semi-analytical formalism they provide. Also, a parallel between HCGs and 1D photonic crystals has been explored in literature [16].

III. DESIGN OF HCG MIRRORS

A. HCGs mirror with broadband reflection

An important property of HCGs is possibility to design a broadband reflection response for integrated mirrors that are also ultra-thin and lightweight compared to other solutions [1].

The design parameters for broadband HCG mirrors are the grating period Λ, the grating thickness t_g and the duty cycle η, whereas the grating refractive index is a given parameter. The first step in design using numerical methods like RCWA is the parameter analysis of the reflection spectrum using scaled parameters. The second step is local optimization using a suitably chosen merit function [21] like the one given in equation below:

$$MF = \frac{\Delta\lambda}{\lambda_0}\frac{1}{N}\sum_{\lambda=\lambda_1}^{\lambda_2} R_{TE(TM)}(\lambda)g(\lambda) \qquad (8)$$

where $\Delta\lambda=\lambda_2-\lambda_1$ is the expected bandwidth around the central wavelength λ_0 which is assumed to be in the middle of the required range, $R(\lambda)$ is the spectral reflectance for a chosen polarization calculated numerically and $g(\lambda)$ is a suitably chosen Gaussian function. Once the optimal parameters of HCGs are found using the chosen local or global algorithm, the tolerances of HCGs parameters can be investigated. In the final step, the structure can be optimized to have not only good efficiency but also large tolerance values.

Interestingly, semi-analytical methods of the coupled mode theory enable physical understanding and efficiency in predesign of broadband reflection [1]. Namely, the nature of HCGs for a specific set of parameters supports only 2 waveguide modes that exist simultaneously in the grating region. These two contra-propagating modes are mutually interfering and can be made to destructively interfere at the exit port of the HCG. In this situation the response is characterized with a very broad bandwidth of high reflectivity. This particular physical picture has been confirmed in literature using similar couple-mode approaches [12]-[15].

We consider a design example of a broadband mirror operating for an TM polarization and formed by silicon bars of refractive index n_g=3.48 and a duty cycle η=0.75, fully immersed in air.

Three distinctive operating regions can be identified with the HCGs: diffraction region, near-wavelength region and deep-sub-wavelength region. In the first region, many diffraction modes beyond zero modes are excited. In the second region HCG parameters are such that the grating is already in the sub-wavelength domain and its response is characterized by excitation of a small number of Bloch (waveguide) modes. This region is most interesting for realization of a high reflectivity broadband response. Finally in the third region the HCG is operating in the deep sub-wavelength domain where only a single propagating mode is excited, the spectral response is without resonance features and the effective mode theory explains well the HCG operation. The reflectivity map shown in Figure 3 can serve as the basis for selecting a suitable period and height (depending on the chosen wavelength) to achieve broadband reflection, which is in this case Λ=0.75 μm, thickness t_g=0.48 μm. The spectral reflectivity for these parameters is shown in Figure 4. The broadband reflectivity is a consequence of interference of the waveguide modes supported by the structure.

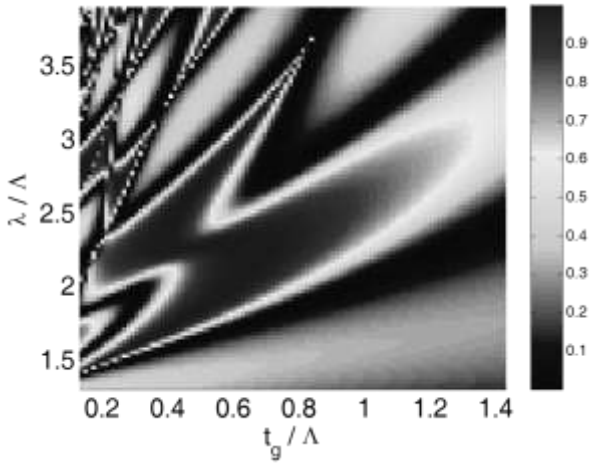

Figure 3 Reflection response dependence on normalized wavelength and grating thickness for TM polarized illumination with normal incidence for a HCG with the duty cycle η=0.75, high index material n_g=3..48 and low index material n_0=1.

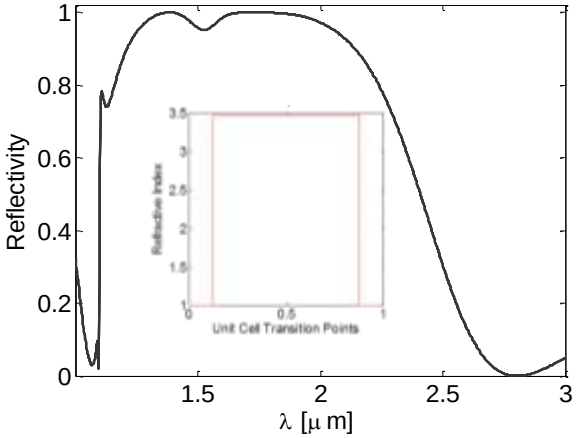

Figure 4. Reflection response (TM polarization, normal incidence) for HCG with the period Λ=0.77 μm, duty cycle η=0.75, thickness tg=0.480 μm, high index material n_g=3..48 and low index material n_0=1.

B. Shaping spectral reflectivity in HCGs mirror with asymmetrical unit cell

The first possible method for tailoring the spectral response is the introduction of defects or asymmetries in the unit cell of

the periodic structure. This strategy already proved successful in controlling the excitation of guided resonances in the case of photonic crystal slabs with aperiodically structured unit cells [22]-[27]. The second method starts with a full aperiodic design for HCG, beyond the unit cell. This approach has been used in photonics and plasmonics to enable tailoring of the spectral response and field profiles [16],[22]. Previously, we analyzed the construction of HCGs with complex unit cells where the topology of the unit cell is derived from a deterministic aperiodic sequence [16].

We consider symmetric and asymmetric perturbations of the periodic structure optimized for broadband reflection, see Fig. 5. We introduce a perturbation of the structure by the re-positioning the transition points in the unit cell

$$x_1^p = x_1^0 - \Delta x;\ x_2^p = x_2^0 + \Delta x; x_{3(4)}^p = x_c \pm \Delta x \quad (9)$$

$$x_c = (x_1^0 + x_2^0)/2\ ;\ \Delta x = p(x_2^0 - x_1^0) \quad (10)$$

where x_n^p represents a new set of transition points in the symmetrically perturbed structure starting from the original transition points x_n^0, Δx is the relative transition point shift with the parameter p describing the relative perturbation calculated with respect to the width of the high index bar, x_c is the central point in the symmetric unit cell. New transition points are calculated in a similar fashion for an asymmetrically perturbed structure with the omission of the perturbation on the one side of the central high index bar. In all cases we keep the total content of the high index material the same between the original and the perturbed structure so that the effective refractive index remains the same.

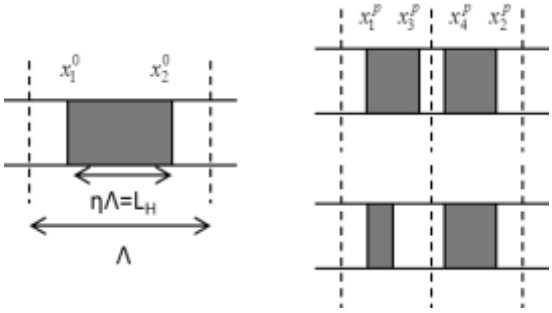

Figure 5. HCG with a symmetrically and an asymmetrically perturbed structure with high index bars on both sides of the center. The unit cell is normalized and the refractive index profile for the transition points between 0 and 1 is depicted.

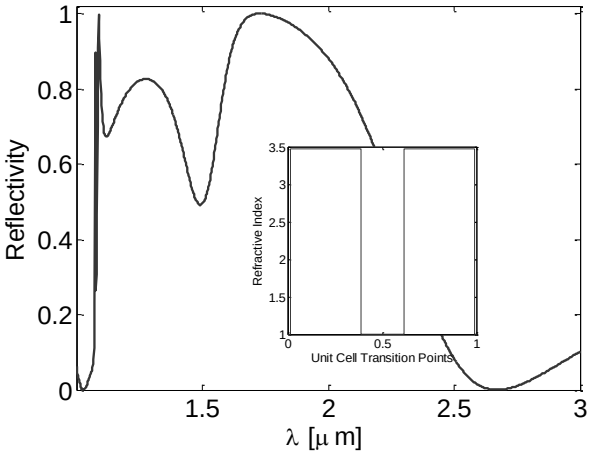

Figure 6. Reflectivity of the HCG with the period Λ=0.77 μm, duty cycle η=0.75, height t_g=0.48 μm, high index material n_g=3.48 (Si) and low index material n_0=1 and a symmetrically perturbed structure with high index bars on both sides of the center and for a relative shift p=0.15. The refractive index distribution in the unit cell is shown in the inset.

We consider a HCG with a period Λ=0.77 μm, duty cycle η=0.75, height t_g=0.48 μm, high index material n_g=3.4.8 (Si) and low index material n_0=1. The reflectivity of the symmetrically perturbed structure is shown in Figure 6: the central high-index region is symmetrically split into 2 parts and moved outwards from the center of the unit cell. The reflectivity is deformed but resonances or similar spectral features are not present in the regions of broadband reflectivity.

The reflectivity of the asymmetrically perturbed structure is shown in Figure 7: the central high index region is symmetrically split into 2 parts and moved outwards from center of the unit cell in asymmetric fashion. High reflectivity is preserved under perturbation, but a resonance appears in the regions of the previously broadband high reflectivity. These very sharp resonances appear even with very small perturbations of the structure. Figure 8 shows a close-up of the reflection resonance and refractive index distribution with the p=0.15.

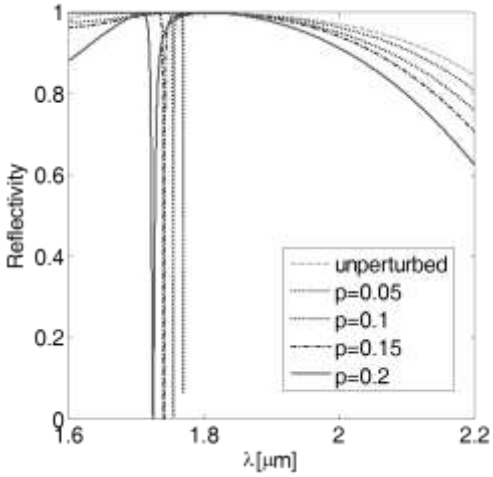

Figure 7 Reflectivity of the HCG with a period Λ=0.77 μm, duty cycle η=0.75, height t_g=0.48 μm, high index material n_g=3.48 (Si) and low index material n_0=1 and asymmetrically perturbed structure with high index bars

on both sides of the center and for different relative shift parameters.

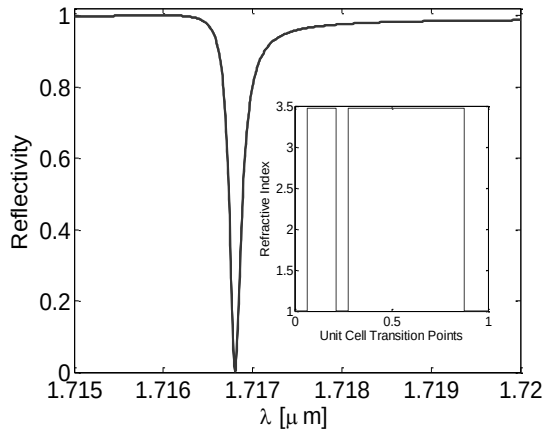

Figure 8 Reflectivity of the HCG with a period Λ=0.77 μm, duty cycle η=0.75, height t_g=0.48 μm, high index material n_g=3.48 (Si) and low index material n_0=1 and asymmetrically perturbed structure with parameter p=0.15. Refractive index distribution is shown in the inset.

The comparison of the spectral response for symmetrically and asymmetrically perturbed structures, like those in Figures 6 and 7, suggests that the spectral response is robust under symmetric unit cell perturbations, while asymmetric unit cell perturbations introduce a new spectral response. In our previous work we showed the examples of highly fragmented spectra present in the case of HCGs with the aperiodic topology in the unit cell [19]. Furthermore, we showed that the systematic use of an aperiodic design of the unit cell enables control of the number of spectral resonances and the symmetry of the fields in the prescribed spectral band [20]. A similar phenomenology related to resonances has been observed in the spectral response of photonic crystals with an aperiodic or defect-based structure [25], [26], [27]. The mechanism responsible for the excitation of these resonances relies on symmetry breaking due to perturbation that opens coupling of the incident wave into the transmitted channel.

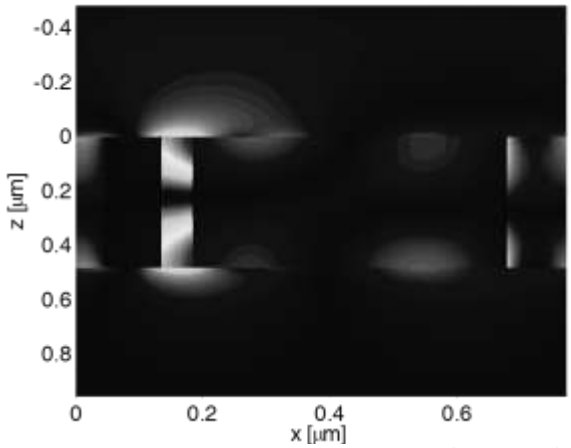

Figure 9 Field distribution at resonance wavelength of 1.716 μm for HCG with the period Λ=0.77 μm, duty cycle η=0.75, height t_g=0.48 μm, high index material n_g=3.48 (Si) and low index material n_0=1 and asymmetrically perturbed structure with parameter p=0.15.

The field distribution of the leading filed component (TM polarization) in the unit cell at the resonance of 1.716 μm is shown in Figure 10. Owing to asymmetry of the unit cell the field distribution is also asymmetric, while showing interesting strong localization in the low index region between two high index bars and with the negligible penetration in the high index material. Hence, field concentration in the region of free space between high index bars makes it accessible for local probing. This is potentially interesting for sensing applications [28]. Beside the reflectivity magnitude, the phase response plays an important role in some devices such as planar focusing mirrors and optical phased arrays described in Section 4. The asymmetric design of the unit cell leads to the appearance of many resonances in the spectral reflection magnitude and phase, as seen in Figure 10.

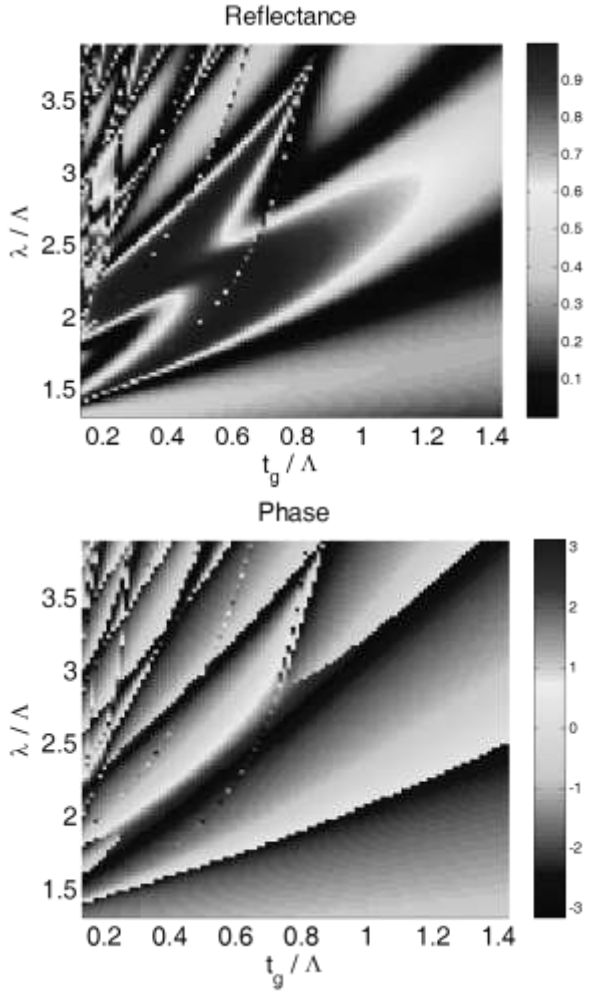

Figure 10 Reflection and phase response of the HCG structure at the wavelength of 1.716 μm with a varying duty cycle for a fixed period Λ=0.77 μm, high index material n_g=3.48 (Si). The asymmetric unit cell structure is the same as in Figure 8.

IV. MEMS MIRRORS WITH SUB-WAVELENGTH HCGS

A. Planar focusing mirrors using non-periodic HCGs

An HCG can be designed to function as an ultrathin planar lens and focusing reflector [1], [8]. This design requires a non-periodic, chirped (sub-wavelength) grating structure enabling control of the reflected beam phase, without changing the high reflectivity of the mirror

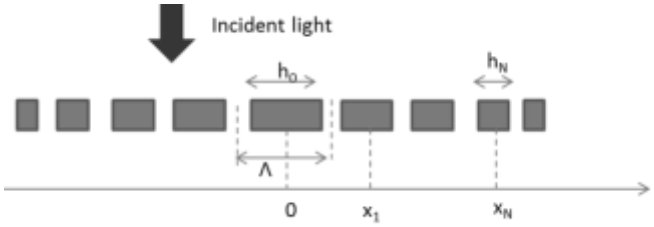

Figure 11 Sketch of the chirped grating structure defining a planar HCG element with spatially varying phase response. The local width of the high index bar is changed within a single unit cell

A design approach is to use scaling of the HCG parameters to shift the desired reflection response at a specified wavelength by scaling the geometrical parameters of the grating. Hence, if the grating has a particular complex reflection coefficient $\mathbf{r}_0$ at a vacuum wavelength λ_0, then a new grating structure with the same reflection coefficient at the wavelength λ scales by the factor $s= \lambda/\lambda_0$, giving $r(\lambda) = \mathbf{r_0}(\lambda/s)=\mathbf{r_0}(\lambda_0)$. Further, the reflection properties of HCGs depend mostly on the local geometry around a specific spatial location. Hence, the non-uniform scaling of the reference grating will lead to local adjustment of the reflection phase while maintaining a large reflectivity at the specified wavelength, see the sketch in Figure 10. If the phase at a certain spatial coordinate is $\varphi(x,y)$ and the non-uniform grating has a slowly varying spatial scale $s(x,y)$, the reflection response is the same as for a periodic structure with reflection $\mathbf{r}_0(\lambda)= \mathbf{r}_0(\lambda/s(x,y))$. In the simplest design approach the base period may be kept constant and only the duty cycle can be changed provided that the phase response is sufficiently variable. A more complex design may use a variation of the base period and also the adjustment of the local thickness of the high index bar. Hence, an algorithm to choose local grating parameters so that the desired phase is reached may be possible using calculation of periodic structures.

The phase variation along the x-axis impressed upon reflected light incident on the chirped grating may lead to strong focusing effect if the phase variation is of the following form:

$$\varphi(x) = \frac{2\pi}{\lambda}\left(f + \frac{\varphi_{max}}{2\pi}\lambda - \sqrt{x^2+f^2}\right) \quad , \qquad (11)$$

where f is the focal length and φ_{max} is the maximum phase change between the middle and the edge of the grating. The continuous phase distribution presented by expression (11) is approximated with the discrete phase distribution defined by the chirped grating.

B. Optical phased arrays using HCGs.

Recently it has been demonstrated that a MEMS mirror with the HCG grating can be used as a phase-tuning element which passively transmits or reflects the incoming light while modifying its phase [1], [9]. Asimple architecture of a MEMS-based phase tuner can be realized by a "piston" mirror approach whereby a mirror is displaced to provide the desired phase shift of reflected light. A sketch of a typical design of the phase tuning element is shown in Figure 12. A high contrast grating mirror is placed in the square frame suspended from thin flexure springs that allow for grating movement. The substrate incorporates (usually) a distributed Bragg reflector (DBR) or possibly a metal mirror. The mirror can be actuated by applying voltage between the contacts at each mirror. Light that falls perpendicularly to the mirror pair is reflected back, but with a phase shift that depends on the mirror separation.

Finally, an array of individually addressable mirrors forms an optical phased array that enables beam steering. The reflection r and the phase of an individual phase tuning element can be simplistically modeled as:

$$r = e^{i\varphi_{HCG}}\frac{|r_{HCG}|-|r_{DBR}|e^{2i\varphi}}{1-|r_{HCG}||r_{DBR}|e^{2i\varphi}} = |r|e^{\,i\Phi} \quad , \qquad (12)$$

where the roundtrip phase is

$$2\varphi = \varphi_{HCG} + \varphi_{DBR} + 2\pi\frac{2(d_0-\Delta d)}{\lambda} \quad , \quad (13)$$

and the resulting phase shift is

$$\Phi = \varphi_{HCG} + 2atan\left(\frac{1+\sqrt{R_{HCG}}}{1-\sqrt{R_{HCG}}}tan\varphi\right) + \pi + 2\pi\frac{2\Delta d}{\lambda} \; . \quad (14)$$

This model takes into account that the HCG mirror is moving and the substrate is stationary. In practice, the total phase shift is usually less than 2π and the reflectance is less than ideal. However, the range of phase element tuning can be addressed additionally with the asymmetric unit cell design. This is due to the fact that phase response is also influenced by resonance induced with the asymmetric unit cell design similar to those discussed in Section 3.

The above design is essentially an all-pass filter (APF) realized as an asymmetric Fabry-Perot (FP) resonator with a carefully designed reflectivity of the top and bottom mirror. When actuating the top mirror to tune the length of the FP resonator across its FP resonance, the reflection phase of the incident light normal to the surface experiences a continuous phase change approaching 2π, while the reflection magnitude is close to unity. The speed of optical phase tuning depends on the mechanical resonance frequency of the HCG MEMS mirror and it allows for very high speed operation owing to the small mass of the HCG compared to other solutions such as DBR mirror. Actual beam steering in the far-field is achieved by creating the desired near-field phase front of the reflected beam on the whole array. Hence, a chip-scale, high-speed, high-integration-density, small-footprint, low-power-consumption operation of this optical phased array is of interest in many applications such as optical circuit switching, light detection and ranging (LIDAR), imaging, sensing, precision targeting etc.

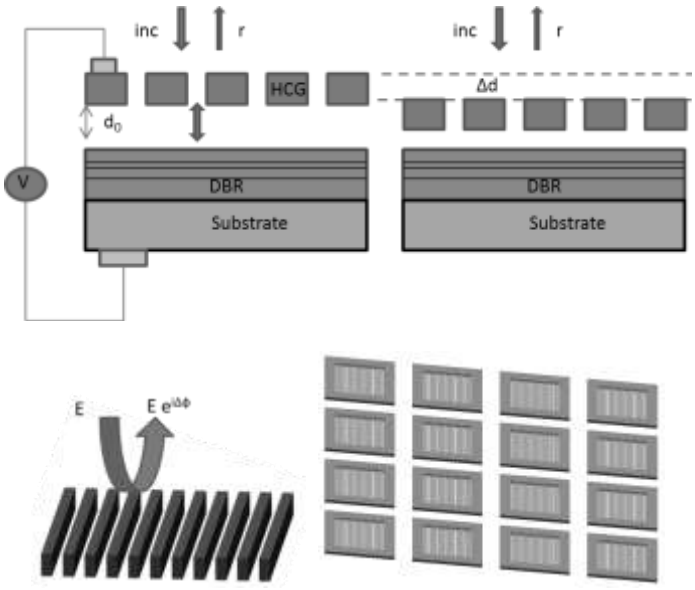

Figure 12 Sketch of a single phase tuning element and a MEMS mirrors array with HCGs for optical phase control.

V. Conclusions

High-contrast gratings (HCG) are important structures in integrated opto-electronics enabled by recent developments in MEMS technology. We showed that the spectral response of HCGs can be tailored via the unit cell perturbations. More specifically, we demonstrated that an asymmetric design of unit cell leads to the appearance of specifically located spectral resonances. We showed that both the magnitude and the phase response are influenced by this asymmetric design. Our results can serve as a guidance for the design of complex HCGs and help with the choice of the efficient initial grating topology prior to global optimization procedure. In addition, they may open more freedom in tailoring amplitude and phase response of the HCG mirrors for specific applications such as high-Q resonance filters, planar focusing elements, beam steering optical phased arrays, etc.

References

[1] C. J. Chang-Hasnain and W. Yang, "High-contrast gratings for integrated optoelectronics", Advances in Optics and Photonics 4, 379–440 (2012).

[2] Y. Rao, W. Yang, C. Chase, M. C. Huang, D. P. Worland, S. Khaleghi, M. R. Chitgarha, M. Ziyadi, A. E. Willner, C. J. Chang-Hasnain, "Long-wavelength VCSEL using high-contrast grating," IEEE J. Sel. Top. Quantum Electron. 19, 1701311 (2013)

[3] Y. Zhou, M. Moewe, J. Kern, M. C. Y. Huang, C. J. Chang-Hasnain, "Surface-normal emission of a high-Q resonator using a subwavelength high-contrast grating," Opt. Express 16(22), 17282–17287 (2008).

[4] A. Ricciardi, S. Campopiano, A. Cusano, T. F. Krauss, L. O'Faolain, "Broadband mirrors in the near-infrared based on subwavelength gratings in SOI." *IEEE* Photonics Journal, 2(5): 696-702, (2010)

[5] Y. WangD. Stellinga, A. B. Klemm, C. P. Reardon, T. F. Krauss, "Tunable Optical Filters Based on Silicon Nitride High Contrast Gratings." IEEE Journal of Selected Topics in Quantum Electronics, vol. 21, no. 4,1-6, (2015)

[6] K. IkedaK. Takeuchi, K. Takayose, I.-S. Chung, J. Mørk, H. Kawaguchi, "Polarization-independent high-index contrast grating and its fabrication tolerances," Appl. Opt. 52, 1049-1053 (2013).

[7] Y. Zhou, V. Karagodsky, B. Pesala, F. G. Sedgwick, C. J. Chang-Hasnain, "A novel ultra-low loss hollow-core waveguide using subwavelength high-contrast gratings.", Optics Express 17.3:1508-1517, (2009)

[8] D. Fattal, J. Li, Z. Peng, M. Fiorentino, and R. G. Beausolei, "Flat dielectric grating reflectors with focusing abilities," Nat. Photonics 4(7), 466–470 (2010).

[9] B.-W. Yoo, M. Megens, T. Chan, T. Sun, W. Yang, C.J. Chang-Hasnain, D.A. Horsley, M.C. Wu, "Optical phased array using high contrast gratings for two dimensional beam forming and beam steering." *Optics Express* 21.10,12238-12248, (2013)

[10] E. Popov, editor, Gratings: Theory and Numeric Applications, Institut Fresnel, CNRS, AMU, 2012

[11] M. Moharam, E. Grann, D. Pommet, and T. Gaylord, "Formulation for stable and efficient implementation of the rigorous coupled-wave analysis of binary gratings," J. Opt. Soc. Am. A 12, 1068-1076 (1995)

[12] P. Lalanne, J.P. Hugonin, P. Chavel, "Optical properties of deep lamellar Gratings: A coupled Bloch-mode insight," IEEE Journal of Lightwave Technology, vol.24, no.6, (2006)

[13] V. Karagodsky, F. Sedgwick, and C. Chang-Hasnain, "Theoretical analysis of sub-wavelength high contrast grating reflectors," Opt. Express 18, 16973-16988 (2010).

[14] V. Karagodsky and C. Chang-Hasnain, "Physics of near-wavelength high contrast gratings," Opt. Express 20, 10888-10895 (2012).

[15] A. Ahmed, M. Liscidini, R. Gordon, "Design and Analysis of High-Index-Contrast Gratings Using Coupled Mode Theory," IEEE Photonics Journal, vol.2, no.6, pp.884-893, (2010)

[16] W. Yang, C. J. Chang-Hasnain, "Physics of high contrast gratings: a band diagram insight", Proc. SPIE 863303 (2013)

[17] O. Solgaard, A.A. Godil, R.T. Howe, L.P. Lee, Y.-A. Peter, H. Zappe, "Optical MEMS: From micromirrors to complex systems.", IEEE Journal of Microelectromechanical Systems, vol. 23 no. 3, 517-538, (2014)

[18] H. Zappe, "Micro-optics: A micro tutorial," Adv. Opt. Technol., vol. 1, no. 3, pp. 117–126, 2012

[19] M. Maksimović, "Modeling and optimization of high index contrast gratings with aperiodic topologies", Proceedings of SPIE Vol. 8789, 87890L (2013)

[20] M. Maksimović, "Resonances in high-contrast gratings with complex unit cell topology", International Workshop on Optical Waveguide Theory and Numerical Modeling (OWTNM 2013), Enschede, The Netherlands, proceedings paper O-1.2, (2013)

[21] C. Chevallier, F. Genty, N. Fressengeas, J. Jacquet, "Robust Design by Antioptimization for Parameter Tolerant GaAs/AlO_x High Contrast Grating Mirror for VCSEL Application." Journal of Lightwave Technology, vol. 31, no. 21 3374-3380, (2013)

[22] E. Maciá, Aperiodic Structures in Condensed Matter: Fundamentals and Applications, CRC Press, (2009)

[23] L. Dal Negro and S.V. Boriskina, "Deterministic aperiodic nanostructures for photonics and plasmonics applications", Laser Photonics Rev., 1–41 (2011)

[24] Maksim Skorobogatiy and Jianke Yang, Fundamentals Of Photonic Crystal Guiding, Cambridge University Press, 2009

[25] O. Kilic, M. Digonnet, G. Kino, and O. Solgaard, "Controlling uncoupled resonances in photonic crystals through breaking the mirror symmetry," Opt. Express 16, 13090-13103 (2008).

[26] I. Gallina, M. Pisco, A. Ricciardi, S. Campopiano, G. Castaldi, A. Cusano, and V. Galdi, "Guided resonances in photonic crystals with point-defected aperiodically-ordered supercells," Opt. Express 17, 19586-19598 (2009).

[27] M. Maksimović, M. Hammer and E. W. C. van Groesen, "Coupled optical defect micro-cavities in one-dimensional photonic crystals and quasi-normal modes", Opt. Eng. 47(11), 114601, (2008)

[28] Z. Jakšić, Micro and Nanophotonics for Semiconductor Infrared Detectors: Towards an Ultimate Uncooled Device, Springer, 2014